Retinoid X Receptor activation prevents diabetic retinopathy in murine models.

Iuliia Dorofeeva[1,a], Assylbek Zhylkibayev[1,a], Irina V. Saltykova[1,a], Venkatram Atigadda[1,b,], Bibek Adhikari[1,a], Oleg Gorbatyuk[1,a], Maria B. Grant[1,c] and Marina Gorbatyuk[1,a]*

[1]University of Alabama at Birmingham, Birmingham, Alabama, USA, Department of Optometry and Vision Science, School of Optometry, [1b,c]Heersink School of Medicine, [b]Department of Dermatology and [c]Department of Ophthalmology and Vision Sciences;

*To whom correspondence should be addressed: Dr. Marina S. Gorbatyuk. Department of Optometry and Vision Science, School of Optometry, University of Alabama at Birmingham. 1670 University Blvd. VH443, Birmingham, Alabama 35233. Tel: 205-934-6762. Fax: 205-934-3425.

Email: mgortk@uab.edu.

Abstract

Previously, the RXR agonist UAB126 demonstrated therapeutic potential to treat obese mice by controlling blood glucose levels (BGL) and altering the expression of genes associated with lipid metabolism and inflammatory response. The purpose of the study was to assess UAB126 effect in progression of diabetic retinopathy (DR) in rodent models of Type1 diabetes (T1D), streptozotocin-induced, and Type2 diabetes (T2D), the db/db mice. UAB126 treatment was delivered either by oral gavage for 6 weeks or by topical application of eye drops for 2 weeks. At the end of the treatment, the retinal function of diabetic mice was assessed by electroretinography (ERG), and their retinal tissue was harvested for protein and gene expression analyses. Bone-marrow cells were isolated and differentiated into bone marrow-derived macrophages (BMDMs). The glycolysis stress test and the 2-DG glucose uptake analysis were performed. Our results demonstrated that in the UAB126-treated diabetic BMDMs, the ECAR rate and the 2-DG uptake were improved as compared to untreated diabetic BMDMs. In UAB126-treated diabetic mice, hyperglycemia was reduced and associated with the preservation of ERG amplitudes and enhanced AMPK activity. Retinas from diabetic mice treated with topical UAB126 demonstrated an increase in Rxr and Ppar, and expression of genes associated with lipid metabolism. Altogether, our data indicate that RXR activation is beneficial to preclinical models of DR.

Introduction

Functioning as a nuclear receptor (NR), the retinoid X receptor (RXR) is a transcriptional factor that binds to the promoter region of genes either as a dimer with itself (homodimer) or with another NR to form a heterodimer. Although RXR can activate transcription as a homodimer, this receptor also serves as an obligatory common dimerization partner for numerous other NRs.[1, 2] The RXR-NR heterodimer binding sequence consists of two six-base pairs sequences.[3]

In general, the molecular structure of RXR is like that of other NRs; RXR proteins contain an A/B region located at the N-terminal, a DNA-binding domain (DBD), and a ligand-binding domain (LBD) positioned at the C-terminal. The role of the A/B domain, while still under investigation, is believed to attract specific binding partners which determines either the activation or repression of the transcriptional complexes.[4] Moreover, nuclear localization sequences are present within the DBD domain of RXR proteins,[5] and in the absence of ligands, RXR can be found both in the cytoplasm and in the nucleus.[6]

RXR occupies a critical position in the NR family because of its ability to form heterodimers with many other family members, and is therefore involved in controlling a myriad of physiologic processes. RXR heterodimers can be classified into two main groups: permissive and non-permissive binding partners. Permissive heterodimers are those that can be activated by the binding of RXR agonists, binding of the agonists of the NR partner, or binding of the agonist to both NRs.[7] Examples of this type of heterodimerization include the RXR/Liver X receptor (LXR), the RXR/Peroxisome proliferator-activated receptor (PPAR), and the RXR/Farnesoid X receptor (FXR) heterodimers.[8] The binding of ligands to both partners could provide an additive or synergistic biological response. Non-permissive heterodimers require that the agonist binds to a the heterodimerization partner while RXR acts as a silent partner. Examples of this heterodimerization include RXR/RAR (retinoid A receptor), RXR/VDR (vitamin D receptor) and RXR/TR (Thyroid hormone receptor).

Overall, three different isoforms of RXR: RXRα, RXRβ, and RXRγ exist. *RXRα* and *RXRβ* mRNAs are widely expressed, whereas *RXRγ* mRNA is restricted to only a few tissues including the retina.[9].[10, 11] RXRα is a predominant isoform that has been identified in the nucleus, cytoplasm, and mitochondria.[12] RXRβ is abundantly expressed in endothelial cells and cancer cell lines and is largely conserved across species.[13] RXRγ is a 14 kB long isoform containing 9 introns widely ranged in size. High RXRγ expression is found in the brain, and its expression is important for development of memory deficit and depression-like behavior upon its ablation.[14]

Mounting evidence indicates that abnormal RXR signaling is involved in neuronal stress and neuroinflammatory response in several neuropathological conditions. RXR protective effects have been established in various cell and animal models, including Alzheimer's, Parkinson's, glaucoma, multiple sclerosis, stroke[13], colitis [15], pulmonary emphysema [16] , and rheumatoid arthritis [17] by modulation of inflammatory responses. [18] In addition, RXRs also control the clearance of apoptotic cells and β-amyloid protein by macrophages; the lack of RXRα impairs the transcription of genes associated with phagocytosis-related events.[19]

Another physiological role of RXR is regulation of lipid metabolism. Bexarotene, an FDA approved rexinoid, improved cholesterol homeostasis and inhibited atherosclerosis progression in a mouse model of dyslipidemia.[20] The level of hepatic gene expression for *Scd1* (stearoyl- Co enzyme A desaturase 1), *Fas* (fatty acid synthase), *Angptl3* (angiopoietin-like 3), *Abaca1 (*ATP-binding cassette subfamily a member 1), and *ApoA-1* (apolipoprotein A1)—was significantly increased in these mice, suggesting improved cholesterol efflux. Despite this fact, RXR activation can increase expression of SREBP-1 leading to elevated triglycerides. [20]

Recently, a novel rexinoid-like molecule UAB126 has been developed.[21, 22] The oral administration of UAB126 reduced obesity, insulin resistance, and dyslipidemia without changes in thyroid hormones.[22] Treatment of mice with UAB126 significantly increased expression of the genes responsible for lipid metabolism and decreased the inflammatory gene expression in white adipose tissue. Interestingly, UAB126 treatment did not raise serum triglyceride levels, and also improved insulin signaling via a decrease in overnight blood glucose and insulin levels.[22]

Overall, the role of RXR in the diseased retina has not been explored carefully, with the exception of the study with rd1 mice that manifested inherited retinal degeneration, or retinitis pigmentosa,[10] that showed that the RXR agonist PA024 decreased photoreceptor cell death.[10]

Given that RXR could be a therapeutic target for degenerating retina, that UAB126 controls lipid metabolism and inflammatory response in obese mice, and that dyslipidemia and inflammation are two critical components of diabetic retinal pathogenesis, we tested UAB126 in two models of DR and demonstrated the therapeutic potential of UAB126 to treat diabetic retinal dysfunction and delay the onset of DR in mice.

Materials and Methods

Animals: Male C57BL/6J (Strain#: 000664) mice, and db/db (BKS.Cg-Dock7m +/+ Leprdb/J; Strain#: 000642) mice were obtained from The Jackson Laboratory and housed in the University of Alabama at

Birmingham (UAB) animal facility, adhering to the guidelines set by the institutional animal care and use committee (UAB-IACUC protocol no. 22104) and the Association for Research in Vision and Ophthalmology guidelines. The mice were kept in a 12-hour light-dark cycle with *ad libitum* access to food and water.

Diabetes Induction: At 8-weeks of age, diabetes was induced by administering five consecutive intraperitoneal injections of 50 mg/kg streptozotocin (STZ) or vehicle (10 mM sodium citrate buffer, ice-cold, pH 4.5). Prior to each STZ injection, the mice underwent a 6-hour food deprivation. Animals were considered diabetic when their blood glucose concentrations exceeded 250 mg/dL on two separate measurements a minimum of two days apart. Throughout the study period, blood glucose levels were monitored weekly, HbA1C and insulin levels were measured at the time of euthanasia. The oral glucose tolerance test was performed as previously described.[23] Animals were euthanized by carbon dioxide following cervical dislocation.

UAB126 Synthesis: The synthesis of UAB126 has been performed as previously described.[22]

Preparation of UAB126 Eye Drops: The nanoemulsion development was carried out using the phase inversion temperature method, as described in the references by Singh et al.[24] and Fernandes et al.[25] In this process, a surfactant mixture comprising Polysorbate-80 (200 mg) and Pluronic-127 (62.5 mg) was heated to a temperature above 70°C and mixed using a magnetic stirrer at 250 rpm for 10 minutes. Once a clear jelly-like liquid was obtained, the active pharmaceutical ingredient UAB-126 (150 mg) was added, and mixing continued until a clear and transparent jelly was formed. Simultaneously, in a separate beaker, 25 ml of water was heated to 70°C, and beta-cyclodextrin (125 mg) and EDTA (6.25 mg) were dissolved in it. This solution was then used for solubilizing the UAB-126 surfactant mixture. Finally, the pH of the solution was adjusted to 7.4 using either 4M sodium hydroxide or diluted hydrochloric acid, as required.

UAB126 Systemic Administration: UAB126 was administered orally in 10% DMSO mixed with corn oil at a dosage of 100 mg/kg, starting a month after the STZ injection, and continued daily for 6 weeks.

UAB126 Topical Application: Ten-week-old db/db animals were used in this experiment. One eye was treated with 10 µl UAB126 eye drops, and fellow eye received same amount of PBS as a Control. Eye drops were applied every day for 2 weeks. After 2 weeks retinas were collected for LC-MS/MS study to detect UAB 126 after the treatment and for RNA isolation following qRT-PCR analysis and Immunohistochemistry.

Retinal Explants: The eyes from C57BL6J animals at postnatal day 8 were enucleated and retina was gently isolated from the eyecup and placed in Neurobasal Serum free medium (Neurobasal-A, 10888022; Invitrogen) containing 2% B27 (0080085-SA; Invitrogen, Carlsbad, CA, USA), 1%N2 (17502-048; Invitrogen), 2 mM GlutaMAX (35050038; Invitrogen), 100 units/mL penicillin–100 lg/mL streptomycin (P4333; Sigma-Aldrich Corp., St. Louis, MO, USA). Retinal explants were maintained at 37°C and 5% CO2 condition. Mannitol (19mM; Control) (Sigma, M4125) and D-glucose 34mM; High glucose) (Sigma, G5767) were dissolved in growth medium. Rexinoid 3, Rexinoid 6 and UAB126 were prepared in sterile water and added to treatment groups with final concentration 100μM. Explants were cultured for 24 hr. and analyzed by using qRT-PCR.

Tissue Homogenization and Extraction for Mass Spectrometry: Kidney, retina, and brain tissues were weighed and homogenized at a density of 140 mg of dry tissue per milliliter in ethyl acetate / isopropanol (4:1) using a Bead Mill 4 homogenizer (Thermo Fisher Scientific, Waltham MA) and 2-mL pre-filled polypropylene microtubes (2.8 mm ceramic beads, 3 x 20 sec cycles, speed 5). Insoluble debris was removed by centrifugation (10,000 x g, 30 min, 5 °C). Fixed aliquots of the supernatants (225 µL) were transferred to clean Eppendorf tubes and evaporated under a gentle stream of nitrogen gas. The residues were reconstituted in 75 µL of methanol/water (4:1), centrifuged (18,000 x g, 30 min, 5 °C), and transferred to 2-mL autosampler vials equipped with low-volume polypropylene inserts and Teflon-lined rubber septa for analysis.

Mass Spectrometry: Retinal samples after systemic UAB126 delivery (oral gavage), and topical application (eyedrops) were sent for LC-MS/MS study. The LC-MS/MS analysis was performed using a Thermo Quantum Ultra triple quadrupole mass spectrometer interfaced to a Waters Acquity UPLC system (Waters Corp, Milford MA). The mass spectrometer was operated in negative ion mode with the following optimized APCI source parameters: corona discharge current 22 µA; ion transfer tube temperature 300°C; vaporizer temperature 290 °C; N2 sheath gas 40; N2 auxiliary gas 5; in-source CID 14. Quantitation was based on MRM detection (UAB-126: m/z 273 → 229, collision energy 15, tube lens 90; Ar collision gas 1.5 mTorr; scan time 100 ms; Q3 scan width 1.0 m/z; Q1/Q3 peak widths at half-maximum 0.7 m/z.). Data acquisition and quantitative spectral analysis were done using Thermo Xcalibur version 2.0.7 SP1 and Thermo LCQuan version 2.7, respectively. Calibration curves were constructed by plotting peak areas against analyte concentrations for a series of nine calibration standards, ranging from 0.375 to 3,750 nmol total analyte. A weighting factor of 1/C2 was applied in the linear least-squares regression analysis to maintain homogeneity of variance across the

concentration range. A kinetic XB-C18 reverse phase analytical column (2.1 x 100 mm, 2.6 µm, Phenomenex, Torrance, CA) was used for all chromatographic separations. Mobile phases were made up of 15 mM ammonium acetate and 0.2 % acetic acid in (A) water/acetonitrile (9:1) and in (B) acetonitrile/methanol/water (90:5:5). Gradient conditions were as follows: 0–1.0 min, B = 40 %; 1–5 min, B = 40–100 %; 5–5.5 min, B = 100 %; 5.5–6 min, B = 100–40 %; 6–10 min, B = 40 %. The flow rate was maintained at 300 µL/min, and the total chromatographic run time was 10 min. A software-controlled divert valve was used to transfer the LC eluent from 0 to 1.5 min of each chromatographic cycle to waste.

Mouse Bone Marrow-Derived Macrophages (BMDM) Generation: Bone marrow cells from the healthy control and diabetic UAB126 treated and untreated mice were isolated by centrifuging bones at >10,000 x g in a microcentrifuge tube for 15 seconds, as previously described.[26] Briefly, we isolated bone-marrow-derived cells, grew them in complete DMEM medium with 10% FBS and 1 IU/mL Pen-Strep, and then differentiated the cells into macrophages by supplementing with M-CSF (20 ng/mL, Peprotech, Rocky Hill, NJ). Seahorse stress testing was performed to compare their metabolic glycolytic activity after 7 days of differentiation.

BMDM Activation and Pro-inflammatory Assessment: On the 7th day of culturing, BMDM were detached using 15mM EDTA in PBS for 10 minutes on ice. The macrophage population was then evaluated by flow cytometry, specifically by examining the expression of CD45/CD11b (double positive) and F4/80 markers, which yielded a percentage of >96%. Subsequently, the detached cells were seeded in 12-well plates and cultured in DMEM supplemented with 10% FBS and 1 IU/mL pen-strep. The following day, non-adherent cells were washed away with PBS, leaving the macrophages behind. The activation process involved adding 200 ng/µL of LPS to the culture media. After 24 hours of conditioning, the media was collected for measurements of pro-inflammatory cytokines using the V-PLEX Proinflammatory Panel 1 Mouse Kit by Meso Scale Diagnostics (K15048D-1, Rockville, MD, USA).

Glucose Uptake Assay: One day before the assay, BMDM cells were seeded in a 24-well plate at a density of $3x10^4$ cells/well. The assay was conducted using both flow cytometry. Positive control cells were treated with Phloretin for 1 hour before the assay. The assay involved exposing the cells to fluorescent 2-deoxy-2-[(7-nitro-2,1,3-benzoxadiazol-4-yl) amino]-D-glucose (2-NBDG) for 30 minutes, following the manufacturer's recommendations (ab287845, Abcam, Waltham, MA, USA). For the flow cytometry analysis, cells were washed, trypsinized, and resuspended in 400 µL of assay buffer.

Glucose uptake was measured using an LSR Fortezza flow cytometer at the UAB Comprehensive Flow Cytometry Core.

Metabolic Stress Test (Seahorse Assay): Resuspended cells were plated in the XF96 tissue culture microplate (Agilent Technologies, Seahorse Bioscience) at a concentration of 3 x 10^5 cells per well in 180 µL of growth media (DMEM with 5.56 mM glucose, 1.0 mM pyruvate, 4 mM L-glutamine, 10% FBS, 1% pen-strep). On the day of the assay, the growth media was removed, and the cells were washed once and replaced with either Glycolytic Stress Test media (phenol-red-free DMEM, with 4 mM glutamine, pH 7.4 at 37°C) or Mito Stress Test media (phenol-red-free DMEM, with 5.56 mM glucose, 1 mM pyruvate, 4 mM glutamine, pH 7.4 at 37°C) to achieve a final volume of 180 µL per well for their respective tests. The cells were then incubated at 37°C in a non-CO2 incubator for 1 hour and subsequently loaded into the Seahorse XFe96 Analyzer (Agilent Technologies, Seahorse Bioscience) when prompted. The Seahorse XF96 sensor cartridge (Agilent Technologies, Seahorse Bioscience) was hydrated in sterile water in a non-CO2 37°C incubator overnight, and then in pre-warmed calibrant in a non-CO2 37°C incubator 1 hour before the assay run. All effectors were prepared to 10x desired concentrations and loaded into the appropriate ports of the sensor cartridge at 20, 22, and 25 µL in ports A, B, and C, respectively, for the Glycolytic Stress Test assay (port A: 100 mM glucose, port B: 15 mM oligomycin, port C: 500 mM 2-DG), and the Mito Stress Test assay (port A: 15 µM oligomycin, port B: 10 µM FCCP, port C: 5 µM each rotenone and antimycin A). The cartridge was then loaded into the Seahorse XFe96 Analyzer, and the protocol was run as follows: calibrate (15 min), equilibrate (15 min), 3 x basal reads (Mix: 3 min, Wait: 0 min, Measure: 3 min), followed by a port injection (A, B, C), each followed by 3 x reads. The extracellular acidification rate (ECAR) was obtained at baseline and in response to each effector injection.

Electroretinography (ERG): The protocol consisted of consecutive scotopic and photopic ERGs (UTAS BigShot ERG instrument, LKC Technologies, Gaithersburg, MD, USA). For scotopic ERG, the mice were dark-adapted for 12 hours, and all subsequent procedures were conducted in a dark room. Anesthesia was induced with an intraperitoneal injection of ketamine/xylazine based on the mice's weight. Topical 2.5% phenylephrine (Paragon BioTeck, Inc., 42702–102-15, Portland, OR, USA) and Gonak (2.5% sterile Hypromellose ophthalmic demulcent solution, AKORN, Lake Forest, IL, USA) was applied to the corneal surfaces. Next, a monopolar contact loop was positioned on the cornea to record the retinal a- and b-wave ERG amplitudes. For scotopic ERG, the mice were exposed to 25 flashes of white LED light with an intensity of 3.14E^{-05} cds/m^2, with 1.5-second intervals between flashes.

Subsequently, a series of 5 flashes was applied at various intensities: 0.025 cds/m^2, 2.5 cds/m^2, 7.91 cds/m^2, and 25 cds/m^2, with 45-second intervals between flashes. Following the scotopic protocol, each mouse was light adapted for 10 minutes under a dome background light of 25 cd/mm. The photopic protocol involved a series of 15 flashes with 1-second intervals between each flash, at intensities of 2.5 cds/m^2, 7.91 cds/m^2, 25 cds/m^2, and 79 cds/m^2. The resulting a- and b-waveforms were analyzed using the LKC EM (LKC Technologies, Gaithersburg, MD, USA).

Immunoblotting: For immunoblotting, mouse retinas were isolated and homogenized using RIPA buffer supplemented with 1% Halt Protease Inhibitor and a phosphatase inhibitor cocktail (Thermo Fisher Scientific, Waltham, MA, USA) and prepared for Western blot as previously described.[27] Protein samples (40–60 µg) were separated by SDS-PAGE and transferred to a PVDF membrane. The anti-phosphorylated AMPK (Cell signaling #2535T, dilution 1:1000) and anti-AMPK (Cell signaling, #5832S, dilution 1:1000) antibodies were used for target protein detection.

Immunohistochemistry: To perform immunohistochemistry (IHC), the eyes were fixed with 4% paraformaldehyde for 4 hours and subsequently preserved in a series of sucrose solutions (15% and 30% sucrose). After preservation, the eyes were washed in 1x PBS and embedded in Tissue-Tek O.C.T. compound (#4583, Sakura Fintek USA, Torrance, CA, USA). The embedded eyes were then frozen in 2-methylbutane at -43°C. IHC analysis was carried out on 12 µm thick retinal sections. The primary anti-RXR antibody (Invitrogen, #433900, dilution 1:200) was used to detect RXR in the human and mouse retinas. Fluorescent confocal microscopy with a Nikon AX-R was performed to take images of retinal sections.

Results

RXR is Reduced in the Diabetic Retinas of Humans and Mice. Immunohistochemical analysis of both human and mouse T2D diabetic retinas (Fig.**1**) depicts reduced RXR staining as compared to age matched controls (human non-DM and db/m mice). Retinal pigment epithelial (RPE), ganglion photoreceptor (Rh) cells showed a marked reduction of RXR.

UAB126 is Present in the Serum and Retina Following Oral Administration. We next analyzed UAB126 levels by LC-MS/MS method in the serum and retinas of mice given UAB126 by gavage. Samples were collected 2h later (**Fig. 2A**). Both the serum and retinal samples had peaks corresponding to UAB126-loaded standard while the samples from the vehicle-treated mice showed no

comparable peaks. These data demonstrate that UAB126 can stay non-metabolized in diabetic mice for at least 2 h and reach the retina upon systemic treatment.

UAB 126 Treatment Reduces Hyperglycemia in Diabetic Mice. Treatment of diabetic mice with UAB126 significantly reduced blood glucose levels although not to normal (**Fig. 2B**). In addition, we found that glucose tolerance was reduced in UAB126 treated diabetic mice at 2 h as compared to untreated group (**Fig. 2C**). In contrast to the improved glucose levels (**Fig. 2D**), insulin did not change in UAB 126 diabetic mice (**Fig. 2E**). This suggests that the treatment primarily regulated insulin receptor levels resulting in enhanced glucose uptake. Both UAB126 treated demonstrated no differencesin body weight (**Fig. 2F**).

UAB126 Treatment Improves the Diminished Retinal Function and Alters Cellular Signaling in Diabetic Retina. Mice were analyzed by scotopic ERG analysis at 6 weeks of treatment. **Figs. 3 A and B** demonstrate that while vehicle-treated diabetic mice showed a reduction in ERG amplitudes, treatment with UAB 126 markedly prevented the decline of A- and B-waves. It is also worth noting that although the B-waves were significantly higher in UAB126-treated vs. untreated groups, the amplitudes did not reach the level of those found in the healthy control delays the progression of vision loss in diabetes.

Western blots of retinas from the experimental cohorts showed a significantly higher level of p-AMPK as compared to vehicle-treated mice.

UAB126 Regulates Metabolism-Relative Biological Pathways in Diabetic Retinas. During DR progression, the diabetic retina experiences monocyte infiltration, which is critical for overall innate immune response and inflammation. Therefore, we next assessed the properties of BMDM macrophages from UAB126-treated mice. BMDM then underwent glycolysis stress test by measuring the extracellular acidification rate (ECAR) using Seahorse approach**. Fig. 4A** demonstrates that the diabetic macrophages derived from vehicle-treated mice showed an increase in the acidification rate after the addition of glycose, oligomycin, and 2-DG as compared to the healthy control group; UAB126 treatment dramatically reduced the ECAR in diabetic macrophages, making their ECAR indistinguishable from healthy macrophages. These data demonstrate that glycolysis in vehicle-treated diabetic macrophages may be enhanced, leading to an increase in lactate efflux. Therefore, we next asked ourselves whether the increase in ECAR could be associated with an increase in glucose uptake by macrophages.

Indeed, a significant (over 2-fold) increase in the uptake of 2-DG labeled with Alexa Flour 488 was detected in the diabetic BMDM from vehicle-treated mice (**Fig. 4B**). Interestingly, treatment with

UAB126 markedly reduced the 2-DG uptake in macrophages. We then analyzed the pro- and anti-inflammatory cytokines in treated macrophages and found that UAB126 treatments led to an increase in IL-10 cytokine while Il-1β was not different between groups of macrophages. (**Fig. 3C**). Overall, the results of the study indicate that UAB216 treatment influenced glucose metabolism in diabetic macrophages as compared to untreated diabetic cells, suggesting that systemic delivery of UAB126 not only reduced BGL and normalized glucose metabolism leading to improved retinal electrophysiology, but also increased the anti-inflammatory program in diabetic macrophages.

Topical Delivery of UAB 126 Activated RXR in Diabetic Retinas. Evaluating the systemic effect of UAB126 treatment on diabetic mice, we wondered whether topically applying eye drops containing the rexinoid could be an effective drug delivery approach. Ocular application of UAB126 drops corneal surface of db/db mice was carried out daily for two weeks.

The LC-MS/MS results demonstrate that the control (untreated) retinas did not contain UAB126-associated peak, and that a strong signal was detected in the retina treated with UAB126 drops (**Fig 5A**). Moreover, RXR staining of the treated retina with anti-RXR antibody demonstrated strong immunoreactivity as compared to buffer-treated retinas (**Fig. 5B**). The increase in the *RXRα* mRNA expression level was also detected in the treated eyes, which was much higher than in untreated diabetic and healthy control group eyes (C57BL6) (**Fig. 5C**). Interestingly, like RXR, PPAR was also reduced in diabetic retinas, and UAB126 treatment also increased its expression level. In addition to the altered expression of two NRs, RXR and PPAR, the expression of genes responsible for lipid metabolism such as *Elovl4, Acly, Fasn, Scd1,* and *Acc1,* was reduced in untreated diabetic retinas and increased upon UAB126 treatment *(p*<0.05), with the exceptions of *Scd1* and *Acc1* genes.

We next decided to assess the ability of other rexinoids to increase PPAR and LXR expression in *ex vivo* experiment. **Fig. 5D** shows that the retinal explants cultured in the media with high glucose (to model diabetic retinopathy) and supplemented with Rexinoid 3 and rexinoid 6[28] demonstrated significant upregulations of *Rxrα*, *Rxrβ,* and *Rxrγ* mRNAs at 24h. We next examined the expression of *Pparα* and *Pparγ* genes and found significant increases in their expression as well.

Discussion

The main findings of this study include that diabetic human and mouse retina exhibit reduced levels of RXR expression in the ONL, INL, RGL and RPE. UAB126 preserves A-wave amplitude and partially protects the B- wave amplitude. This indicates the protection of retinal function, an effect that could be mediated by the reduction in glucose in the UAB126 treated diabetic mice. *In vitro* studies with

bone marrow-derived macrophages from the diabetic untreated and UAB treated mice demonstrate that UAB126 treatment increased expression of the anti-inflammatory cytokine IL-10. Direct ocular delivery in T2D mice using topical UAB126 application resulted in an increase in retinal mRNA for Rxrα, Pparα, and lipid-associated gene expression. Collectively, our data support the beneficial effect of RXR agonism on the neural retina by modulation of glucose metabolism, and by increasing expression of the key anti-inflammatory cytokine IL-10. These findings suggest that RXR represents a novel target for the DR treatment.

The previous study in obese mice showed that UAB126 can control glucose levels; both glucose and HbA1C levels were reduced in our study. These data imply that UAB126 could be beneficial to diabetic patients not only by maintaining the blood glucose and therefore managing the progression of diabetes, but also by directly altering the biological processes in diabetic retinas. Our studies suggest that UAB126 treatment reprograms cellular metabolism in macrophages, modifying glycolysis and glucose consumption rates. The UAB126 treated macrophages responded to all steps of metabolic stress similar to cells isolated from healthy mice. The response of macrophages to metabolic stress has been controversial. Zeng et al. proposed that glycolysis is upregulated in C57BL6 BMDM under high glucose conditions[29] and the ECAR rate is enhanced in adipose tissue macrophages derived from obese mice.[30, 31] In contrast, peritoneal macrophages isolated from STZ-induced diabetic $Ldr^{-/-}$ mice manifest suppressed glucose uptake and glycolysis[32] and the results by Pavlou et al. proposed that long-term exposure of C57BL6 BMDM in medium supplemented with high glucose suppresses the ECAR rate.[33] The controversy could be explained by difference in the mouse strains, sources of isolated macrophage, the conditions of treatment, and *in vitro* vs. *in vivo* glucose exposures. However, the importance of metabolic shift in diabetic macrophages is widely recognized. It has been proposed that M1 macrophages rely mainly on glycolysis and that their aberrant TCA cycle leads to the accumulation of succinate, which in turn induces HIF1α stabilization and activates the transcription of glycolytic genes which sustain glycolytic metabolism.[34] In contrast, M2 macrophages depend on oxidative phosphorylation, and their TCA cycle is intact. Together, these data suggest that the metabolic state of macrophages could determine their polarization. The LPS-treated macrophages from UAB126-fed diabetic mice showed increased concentration of anti-inflammatory IL-10 cytokine, which in general is known to be a M2 marker.[35] This result implies that during the course of diabetes, infiltrating monocytes may have become M2-type macrophages in the UAB126 treated diabetic retina as compared to the untreated. In line with the upregulated ECAR rate, we also observed reduced glucose consumption in UAB126 treated diabetic macrophages. While the mechanism by which UAB126

reduces serum glucose remains to be elucidated, the effect may be indirect by modulation of inflammatory signaling which in turn could influence the insulin pathway.[36] However, interpretation of the studies needs to be considered in the context of T1D vs. T2D. The dual activation of RXR and PPAR by RXR agonist such as UAB126 supports the feasibility of UAB126 RXR agonist in treatment of T2D.[36] Specifically, insulin receptors may be desensitized in retinas of T2D mice. Thus, UAB126 could help balance glucose uptake by retinal cells, which improves insulin-controlled rhodopsin signaling and restores diminished retinal function.[37]

In support of this hypothesis, we found that the 6-week treatment of diabetic mice prevents the decline of retinal function. These data suggest that the vision deficit in treated diabetic mice is slowed down. Moreover, the increase in the p-AMPK level in treated diabetic retinas indicate a metabolic shift towards homeostasis. It has been demonstrated that diabetes-induced inflammation strongly correlates with a reduced AMPK pathway, the downregulation of which leads to diminished SIRT1 activation.[38] AMPK stimulation is known to prevent photoreceptor cell degeneration in T1D mice.[39] Therefore, an increase in AMPK activity may indicate the reduced inflammatory response and diminished photoreceptor functional loss. This data correlate with the observed reduction in the decline of A-wave scotopic amplitudes in UAB126-treated diabetic mice vs. untreated ones. Given that BGL is reduced, insulin is not changed, and AMPK activity is increased in UAB126-treated animal tissues, it is possible that RXR-based therapy provides effects like metformin in T2D patients.[40]

The clinical importance of the eye drops containing effective drugs such as UAB 126 to correct DR has marked translational significance as a way of delivering bioactive compounds on a daily basis. The topical application of UAB126 successfully delivered the drug to the retina and increased the expression of genes responsible for lipid metabolism. This suggests that UAB126 application could normalize local lipid synthesis. Thus, the reduced expression of *Elovl2* and *Elovl4*, elongases required for the biosynthesis of long-chain polyunsaturated fatty acids, occurs in diabetic retinas.[41, 42] Their increase could help to slow down retinal pathogenesis by producing complex lipids known to be diminished in diabetic retinas overall.[43] Future studies should overcome the limitations of the present research, and identify the modified lipid profile in UAB126-treated diabetic retinas. Moreover, the screening and the validation of new efficient rexinoids should be continued to move the field towards their clinical application to treat DR. In our study, both rexinoid 3 and rexinoid 6 not only significantly increased all three RXR isoforms in the retina exposed to high glucose, but also dramatically enhanced PPARα and PPARγ, which are known to control inflammation in diabetic retinas.[44]

One of the key issues of contemporary biology and the field studying NRs is whether RXR provides a separable response and whether a RXR homodimer can function as a biological relevant transcription unit. In our study, RXR increase was accompanied by an increase in PPARs and LXR, non-permissive RXR binding partners. Therefore, it is important to understand how the pleotropic effects of rexinoids are carried out. Future research identifying binding partners activated by UAB126 treatment and their requirements to form an active RXR/NR heterodimer to provide a therapeutic effect should be conducted. These studies could not only overcome the limitations of the current research, but also provide a link between rexinoids and cellular signaling activated by UAB126 treatment.

In conclusion, our studies support the therapeutic potential of rexinoids to treat DR. In sum, our data indicate that systemic RXR-based therapy could benefit diabetic patients not only by reducing the BGL, and therefore controlling DR progression, but also by altering local retinal metabolism and the inflammatory response.

Acknowledgment.

The study was supported by the NIH grants: NEI R01027763, P30 EY003039, IDDK DK P30DK079626, NIDDK DK056336. The authors would like to thank Dr. Mohamed Al-Shabrawey at Oakland University for sharing the sections of human diabetic cryopreserved retinas, Dr. Melissa J. Sammy at the UAB Bioanalytical Redox Biology Core for her assistance with Seahorse metabolic stress, Dr. Vidya Sagar Hanumanthu at the UAB Comprehensive Flow Cytometry Core for his assistance with flow cytometry, Heather Lynn Hunter at the UAB Nutrition Obesity Research Center for the measurement of mouse insulin, and Dr. Wade Calcutt at the Mass Spectrometry Core Facility at Vanderbilt University for detection of UAB126 by LC-MS/MS.

Figure Legends:

Figure 1. Expression of RXR in human and mouse diabetic retinas. **A**: Immunostaining of human retinas comparing control (left) and diabetic (right) samples reveals reduced RXR expression (in green) in the outer nuclear layer (ONL), inner nuclear layer (INL), and retinal ganglion cell layer (RGL) of diabetic retinas. The nuclei are shown in red. **B** and **C**: Immunostaining of db/db mouse retinas, a T2D mouse model, demonstrates decreased RXR expression in retinal ganglion cells (RGC), inner nuclear layer (INL), outer nuclear layer (ONL), and retinal pigment epithelial cells (RPE), consistent with the findings in human diabetic retinas.

Figure 2. The oral administration of UAB126 in the diabetic retina. **A:** LC-MS/MS analysis shows the detection of the RXR agonist, UAB126, in the serum and retinas of mice after systemic delivery. Representative LC-MS/MS peaks are presented. **B**: Diabetic mice treated with UAB126 for 6 weeks display a reduction in blood glucose levels (BGL) compared to diabetic controls (n=3-6). The average of 6-week BGL measurements is shown. **C:** The oral glucose tolerance test conducted in diabetic mice at the end of the UAB126 treatment; the UAB126 treatments reduced the blood glucose level in diabetic mice at 2h after the oral glucose load, demonstrating the partial clearance of glucose from the body. Untreated diabetic mice, however, showed no difference in the clearance. **D.** The decrease in BGL correlates with HbA1C measurements, indicating the beneficial effects of UAB126 treatment on glycemic control at 6 weeks. **E:** UAB126 treatment does not alter insulin levels, showing that the compound does not affect insulin secretion in diabetic mice. **F:** The treatment of diabetic mice with UAB126 does not lead to significant body weight loss compared to untreated diabetic mice (n=5). ***p < 0.001, and ****p < 0.0001.

Figure 3. Treatment of diabetic mice with UAB126 prevents retinal function loss. **A**: Electroretinogram (ERG) recordings from diabetic retinas show reduced A-wave amplitudes (photoreceptor responses) and B-wave amplitudes (bipolar and Muller cell responses) compared to healthy control retinas at 14 weeks after streptozotocin (STZ) injection. Treatment with UAB126 preserves the A-wave amplitude and partially protects the B-wave amplitude decline, indicating protection of retinal function. **B:** Representative ERG waveforms from healthy control, diabetic + vehicle, and diabetic +UAB126-treated mice are shown. **C**: The improvement in retinal function in UAB126-treated diabetic retinas is associated with an increase in AMPK activation (n=5-6). *p < 0.05, **p < 0.01.

Figure 4. The UAB126 treatment normalizes metabolism in bone marrow-derived macrophages. **A:** Glycolytic stress test measures the extracellular acidification rate (ECAR) at each step of glucose, oligomycin, and 2-DG addition (n=3-4). No difference is observed between control and UAB126-treated macrophages. However, significant differences are observed between vehicle-treated diabetic and UAB126-treated diabetic or vehicle-treated and the control group at all steps of ECAR (*** p<0.001). Results were analyzed by two-way ANOVA. **B:** UAB126-treated macrophages show a lower rate of 2-DG (2-deoxyglucose) uptake compared to vehicle-treated macrophages, although not reaching the level of healthy untreated control macrophages. **C:** UAB126-treated macrophages express increased levels of Il-10 mRNA, a biomarker of M2 macrophages, while Il-1β mRNA expression remains unchanged (n=3-4). **p < 0.01, ***p < 0.001, and ****p < 0.0001.

Figure 5. The eye drops containing UAB126 were designed for topical application and retinal delivery of rexinoids. **A:** LC-MS/MS analysis confirms the accumulation of UAB126 in the retinas after topical application of eye drops. LC-MS/MS spectrograms show UAB126-treated retinas compared to untreated controls. **B**: Immunostaining of control (left) and diabetic (right) retinas with anti-RXR antibody detects the RXR signal (in green) following topical UAB126 application. **C:** Topical UAB126 application results in an increase in Rxrα, Pparα, and lipid-associated gene expression in db/db retinas, suggesting altered lipid metabolism in treated diabetic retinas (n=3-5). **D**: Retinal explants cultured in high glucose medium as compared to control (mannitol) exhibit decreased expression of Rxrα, Pparα, and Lxrβ mRNA. **E**: Treatment with UAB126 in high glucose medium increases the expression of these genes (n=3-4). **F**: The application of other rexinoids (rexinoid 3 and rexinoid 6) to C57BL6 retinal explants exposed to high glucose results in a dramatic increase in all three RXR isoforms (n=3-4). **G**: In addition to RXR, UAB126 treatment induces an increase in *Pparα* and *Pparγ* mRNA expression, suggesting potential interactions and effects on other binding partners for RXR-based therapy (n=4). *p < 0.05, **p < 0.01, ***p < 0.001, and ****p < 0.0001.

1. Zhang XK, Lehmann J, Hoffmann B, et al. Homodimer formation of retinoid X receptor induced by 9-cis retinoic acid. *Nature* 1992;358:587-591.

2. Osz J, Brelivet Y, Peluso-Iltis C, et al. Structural basis for a molecular allosteric control mechanism of cofactor binding to nuclear receptors. *Proc Natl Acad Sci U S A* 2012;109:E588-594.

3. Chambon P. A decade of molecular biology of retinoic acid receptors. *FASEB J* 1996;10:940-954.

4. Huang P, Chandra V, Rastinejad F. Retinoic acid actions through mammalian nuclear receptors. *Chem Rev* 2014;114:233-254.

5. Gocek E, Baurska H, Marchwicka A, Marcinkowska E. Regulation of Leukemic Cell Differentiation through the Vitamin D Receptor at the Levels of Intracellular Signal Transduction, Gene Transcription, and Protein Trafficking and Stability. *Leuk Res Treatment* 2012;2012:713243.

6. Yasmin R, Williams RM, Xu M, Noy N. Nuclear import of the retinoid X receptor, the vitamin D receptor, and their mutual heterodimer. *J Biol Chem* 2005;280:40152-40160.

7. Szeles L, Poliska S, Nagy G, et al. Research resource: transcriptome profiling of genes regulated by RXR and its permissive and nonpermissive partners in differentiating monocyte-derived dendritic cells. *Mol Endocrinol* 2010;24:2218-2231.

8. Kubickova B, Martinkova S, Bohaciakova D, et al. Effects of all-trans and 9-cis retinoic acid on differentiating human neural stem cells in vitro. *Toxicology* 2023;487:153461.

9. Sugawara A, Yen PM, Qi Y, Lechan RM, Chin WW. Isoform-specific retinoid-X receptor (RXR) antibodies detect differential expression of RXR proteins in the pituitary gland. *Endocrinology* 1995;136:1766-1774.

10. Volonte YA, Ayala-Pena VB, Vallese-Maurizi H, et al. Retinoid X receptor activation promotes photoreceptor survival and modulates the inflammatory response in a mouse model of retinitis pigmentosa. *Biochim Biophys Acta Mol Cell Res* 2021;1868:119098.

11. Roberts MR, Hendrickson A, McGuire CR, Reh TA. Retinoid X receptor (gamma) is necessary to establish the S-opsin gradient in cone photoreceptors of the developing mouse retina. *Invest Ophthalmol Vis Sci* 2005;46:2897-2904.

12. UniProt C. UniProt: the universal protein knowledgebase in 2021. *Nucleic Acids Res* 2021;49:D480-D489.

13. Sharma S, Shen T, Chitranshi N, et al. Correction to: Retinoid X Receptor: Cellular and Biochemical Roles of Nuclear Receptor with a Focus on Neuropathological Involvement. *Mol Neurobiol* 2022;59:2051.

14. Wietrzych-Schindler M, Szyszka-Niagolov M, Ohta K, et al. Retinoid x receptor gamma is implicated in docosahexaenoic acid modulation of despair behaviors and working memory in mice. *Biol Psychiatry* 2011;69:788-794.

15. Matsumoto R, Takahashi D, Watanabe M, et al. A Retinoid X Receptor Agonist Directed to the Large Intestine Ameliorates T-Cell-Mediated Colitis in Mice. *Front Pharmacol* 2021;12:715752.

16. Morichika D, Miyahara N, Fujii U, et al. A retinoid X receptor partial agonist attenuates pulmonary emphysema and airway inflammation. *Respir Res* 2019;20:2.

17. Li Y, Xing Q, Wei Y, et al. Activation of RXR by bexarotene inhibits inflammatory conditions in human rheumatoid arthritis fibroblast-like synoviocytes. *Int J Mol Med* 2019;44:1963-1970.

18. Nunez V, Alameda D, Rico D, et al. Retinoid X receptor alpha controls innate inflammatory responses through the up-regulation of chemokine expression. *Proc Natl Acad Sci U S A* 2010;107:10626-10631.

19. Roszer T, Menendez-Gutierrez MP, Cedenilla M, Ricote M. Retinoid X receptors in macrophage biology. *Trends Endocrinol Metab* 2013;24:460-468.

20. Lalloyer F, Fievet C, Lestavel S, et al. The RXR agonist bexarotene improves cholesterol homeostasis and inhibits atherosclerosis progression in a mouse model of mixed dyslipidemia. *Arterioscler Thromb Vasc Biol* 2006;26:2731-2737.

21. Grubbs CJ, Hill DL, Bland KI, et al. 9cUAB30, an RXR specific retinoid, and/or tamoxifen in the prevention of methylnitrosourea-induced mammary cancers. *Cancer Lett* 2003;201:17-24.

22. Ren G, Kim T, Kim HS, et al. A Small Molecule, UAB126, Reverses Diet-Induced Obesity and its Associated Metabolic Disorders. *Diabetes* 2020;69:2003-2016.

23. Melo da Cunha JDS, Alfredo TM, Dos Santos JM, et al. Antioxidant, antihyperglycemic, and antidiabetic activity of Apis mellifera bee tea. *PLoS One* 2018;13:e0197071.

24. Singh Y, Meher JG, Raval K, et al. Nanoemulsion: Concepts, development and applications in drug delivery. *J Control Release* 2017;252:28-49.

25. Fernandes AR, Sanchez-Lopez E, Santos TD, Garcia ML, Silva AM, Souto EB. Development and Characterization of Nanoemulsions for Ophthalmic Applications: Role of Cationic Surfactants. *Materials (Basel)* 2021;14.

26. Amend SR, Valkenburg KC, Pienta KJ. Murine Hind Limb Long Bone Dissection and Bone Marrow Isolation. *J Vis Exp* 2016.

27. Saltykova IV, Elahi A, Pitale PM, Gorbatyuk OS, Athar M, Gorbatyuk MS. Tribbles homolog 3-mediated targeting the AKT/mTOR axis in mice with retinal degeneration. *Cell Death Dis* 2021;12:664.

28. Atigadda VR, Kashyap MP, Yang Z, et al. Conformationally Defined Rexinoids for the Prevention of Inflammation and Nonmelanoma Skin Cancers. *J Med Chem* 2022;65:14409-14423.

29. Zeng H, Qi X, Xu X, Wu Y. TAB1 regulates glycolysis and activation of macrophages in diabetic nephropathy. *Inflamm Res* 2020;69:1215-1234.

30. Sharma M, Boytard L, Hadi T, et al. Enhanced glycolysis and HIF-1alpha activation in adipose tissue macrophages sustains local and systemic interleukin-1beta production in obesity. *Sci Rep* 2020;10:5555.

31. Serbulea V, Upchurch CM, Schappe MS, et al. Macrophage phenotype and bioenergetics are controlled by oxidized phospholipids identified in lean and obese adipose tissue. *Proc Natl Acad Sci U S A* 2018;115:E6254-E6263.

32. Matsuura Y, Shimizu-Albergine M, Barnhart S, et al. Diabetes Suppresses Glucose Uptake and Glycolysis in Macrophages. *Circ Res* 2022;130:779-781.

33. Pavlou S, Lindsay J, Ingram R, Xu H, Chen M. Sustained high glucose exposure sensitizes macrophage responses to cytokine stimuli but reduces their phagocytic activity. *BMC Immunol* 2018;19:24.

34. Viola A, Munari F, Sanchez-Rodriguez R, Scolaro T, Castegna A. The Metabolic Signature of Macrophage Responses. *Front Immunol* 2019;10:1462.

35. Cantero-Navarro E, Rayego-Mateos S, Orejudo M, et al. Role of Macrophages and Related Cytokines in Kidney Disease. *Front Med (Lausanne)* 2021;8:688060.

36. Cesario RM, Klausing K, Razzaghi H, et al. The rexinoid LG100754 is a novel RXR:PPARgamma agonist and decreases glucose levels in vivo. *Mol Endocrinol* 2001;15:1360-1369.

37. Rajala A, Teel K, Bhat MA, et al. Insulin-like growth factor 1 receptor mediates photoreceptor neuroprotection. *Cell Death Dis* 2022;13:613.

38. Kubota S, Ozawa Y, Kurihara T, et al. Roles of AMP-activated protein kinase in diabetes-induced retinal inflammation. *Invest Ophthalmol Vis Sci* 2011;52:9142-9148.

39. Song S, Bao S, Zhang C, et al. Stimulation of AMPK Prevents Diabetes-Induced Photoreceptor Cell Degeneration. *Oxid Med Cell Longev* 2021;2021:5587340.

40. Freemark M, Bursey D. The effects of metformin on body mass index and glucose tolerance in obese adolescents with fasting hyperinsulinemia and a family history of type 2 diabetes. *Pediatrics* 2001;107:E55.

41. Wang Q, Tikhonenko M, Bozack SN, et al. Changes in the daily rhythm of lipid metabolism in the diabetic retina. *PLoS One* 2014;9:e95028.

42. Tikhonenko M, Lydic TA, Wang Y, et al. Remodeling of retinal Fatty acids in an animal model of diabetes: a decrease in long-chain polyunsaturated fatty acids is associated with a decrease in fatty acid elongases Elovl2 and Elovl4. *Diabetes* 2010;59:219-227.

43. Fort PE, Rajendiran TM, Soni T, et al. Diminished retinal complex lipid synthesis and impaired fatty acid beta-oxidation associated with human diabetic retinopathy. *JCI Insight* 2021;6.

44. Yuan T, Dong L, Pearsall EA, Zhou K, Cheng R, Ma JX. The Protective Role of Microglial PPARalpha in Diabetic Retinal Neurodegeneration and Neurovascular Dysfunction. *Cells* 2022;11.

Figure 1

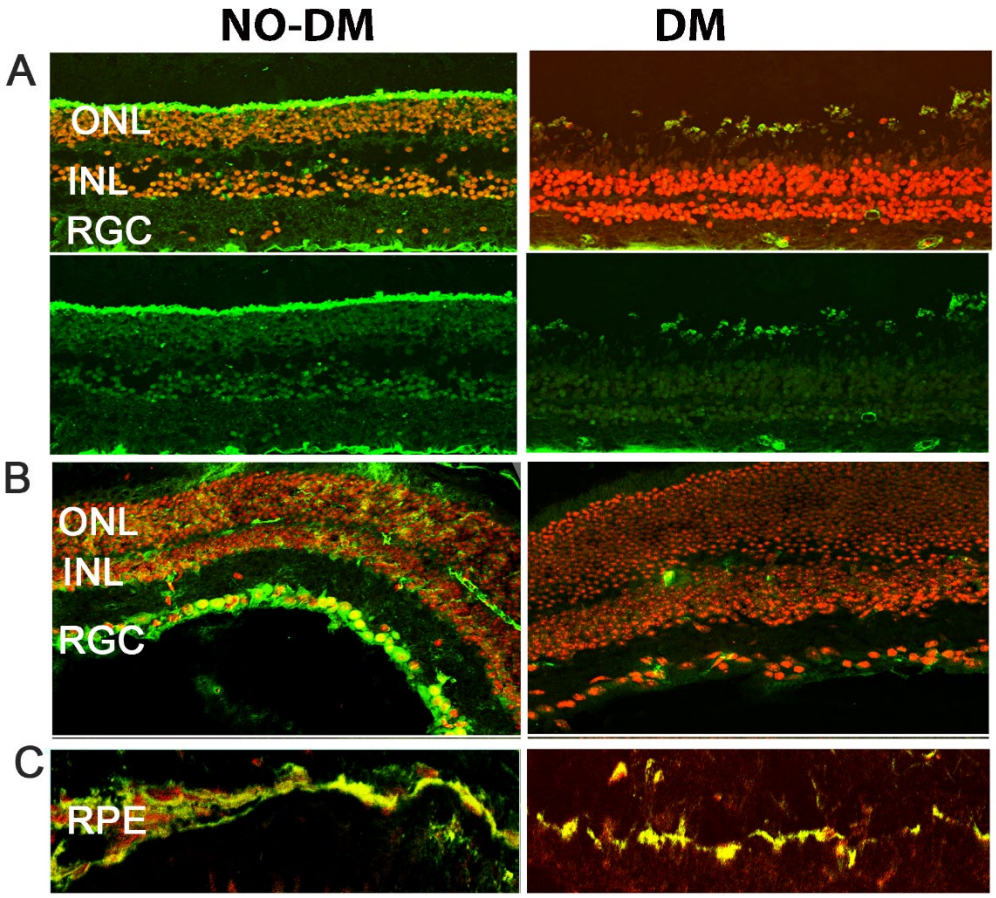

Figure 1. Expression of RXR in human and mouse diabetic retinas. **A**: Immunostaining of human retinas comparing control (left) and diabetic (right) samples reveals reduced RXR expression (in green) in the outer nuclear layer (ONL), inner nuclear layer (INL), and retinal ganglion cell layer (RGL) of diabetic retinas. The nuclei are shown in red. **B** and **C**: Immunostaining of db/db mouse retinas, a T2D mouse model, demonstrates decreased RXR expression in retinal ganglion cells (RGC), inner nuclear layer (INL), outer nuclear layer (ONL), and retinal pigment epithelial cells (RPE), consistent with the findings in human diabetic retinas.

Figure 2

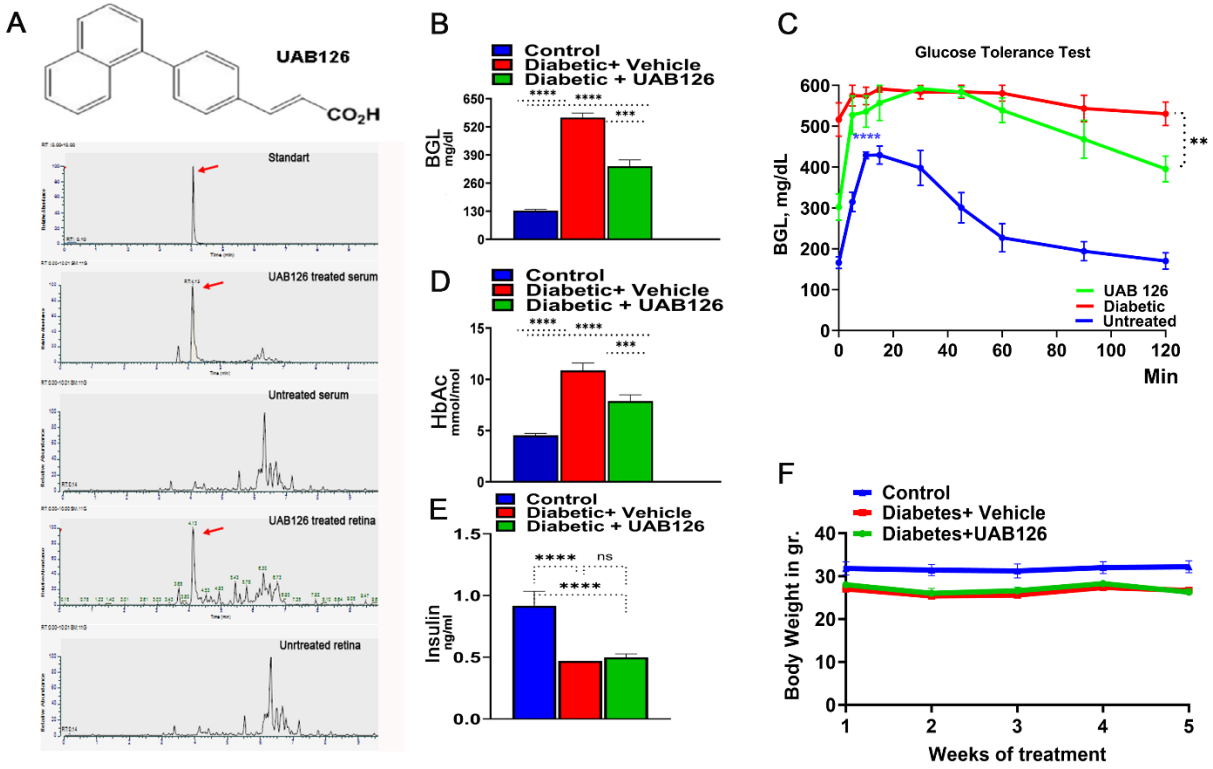

Figure 2. The oral administration of UAB126 in the diabetic retina. **A:** LC-MS/MS analysis shows the detection of the RXR agonist, UAB126, in the serum and retinas of mice after systemic delivery. Representative LC-MS/MS peaks are presented. **B**: Diabetic mice treated with UAB126 for 6 weeks display a reduction in blood glucose levels (BGL) compared to diabetic controls (n=3-6). The average of 6-week BGL measurements is shown. **C:** The oral glucose tolerance test conducted in diabetic mice at the end of the UAB126 treatment; the UAB126 treatments reduced the blood glucose level in diabetic mice at 2h after the oral glucose load, demonstrating the partial clearance of glucose from the body. Untreated diabetic mice, however, showed no difference in the clearance. **D.** The decrease in BGL correlates with HbA1C measurements, indicating the beneficial effects of UAB126 treatment on glycemic control at 6 weeks. **E:** UAB126 treatment does not alter insulin levels, showing that the compound does not affect insulin secretion in diabetic mice. **F:** The treatment of diabetic mice with UAB126 does not lead to significant body weight loss compared to untreated diabetic mice (n=5). ***p < 0.001, and ****p < 0.0001.

Figure 3

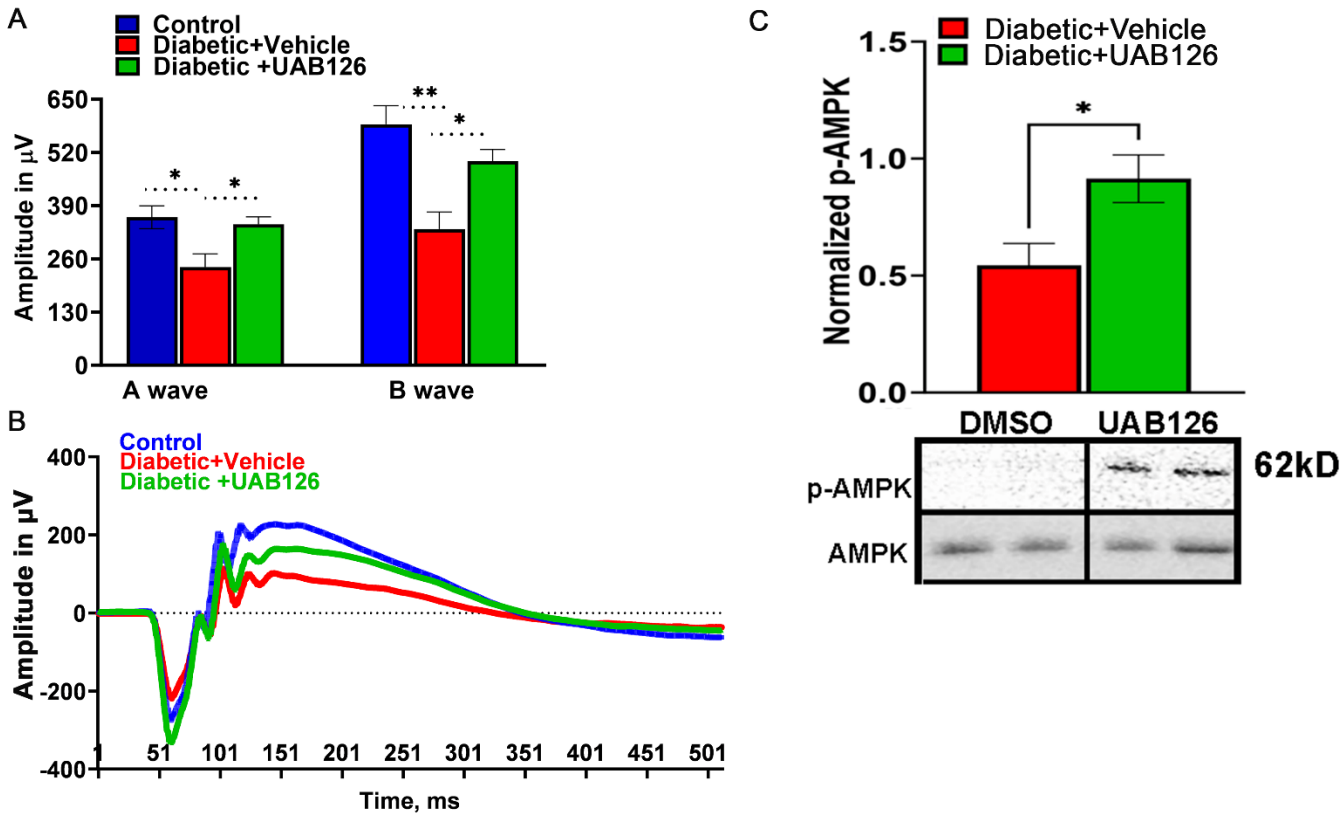

Figure 3. Treatment of diabetic mice with UAB126 prevents retinal function loss. **A**: Electroretinogram (ERG) recordings from diabetic retinas show reduced A-wave amplitudes (photoreceptor responses) and B-wave amplitudes (bipolar and Muller cell responses) compared to healthy control retinas at 14 weeks after streptozotocin (STZ) injection. Treatment with UAB126 preserves the A-wave amplitude and partially protects the B-wave amplitude decline, indicating protection of retinal function. **B:** Representative ERG waveforms from healthy control, diabetic + vehicle, and diabetic +UAB126-treated mice are shown. **C**: The improvement in retinal function in UAB126-treated diabetic retinas is associated with an increase in AMPK activation (n=5-6). *p < 0.05, **p < 0.01.

Figure 4

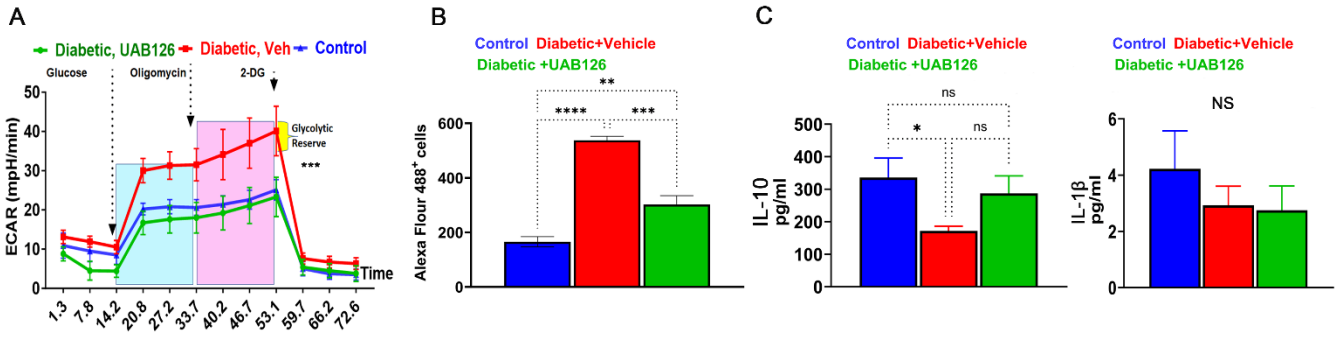

Figure 4. The UAB126 treatment normalizes metabolism in bone marrow-derived macrophages. **A:** Glycolytic stress test measures the extracellular acidification rate (ECAR) at each step of glucose, oligomycin, and 2-DG addition (n=3-4). No difference is observed between control and UAB126-treated macrophages. However, significant differences are observed between vehicle-treated diabetic and UAB126-treated diabetic or vehicle-treated and the control group at all steps of ECAR (*** $p<0.001$). Results were analyzed by two-way ANOVA. **B:** UAB126-treated macrophages show a lower rate of 2-DG (2-deoxyglucose) uptake compared to vehicle-treated macrophages, although not reaching the level of healthy untreated control macrophages. **C:** UAB126-treated macrophages express increased levels of Il-10 mRNA, a biomarker of M2 macrophages, while Il-1β mRNA expression remains unchanged (n=3-4). **$p < 0.01$, ***$p < 0.001$, and ****$p < 0.0001$.

Figure 5

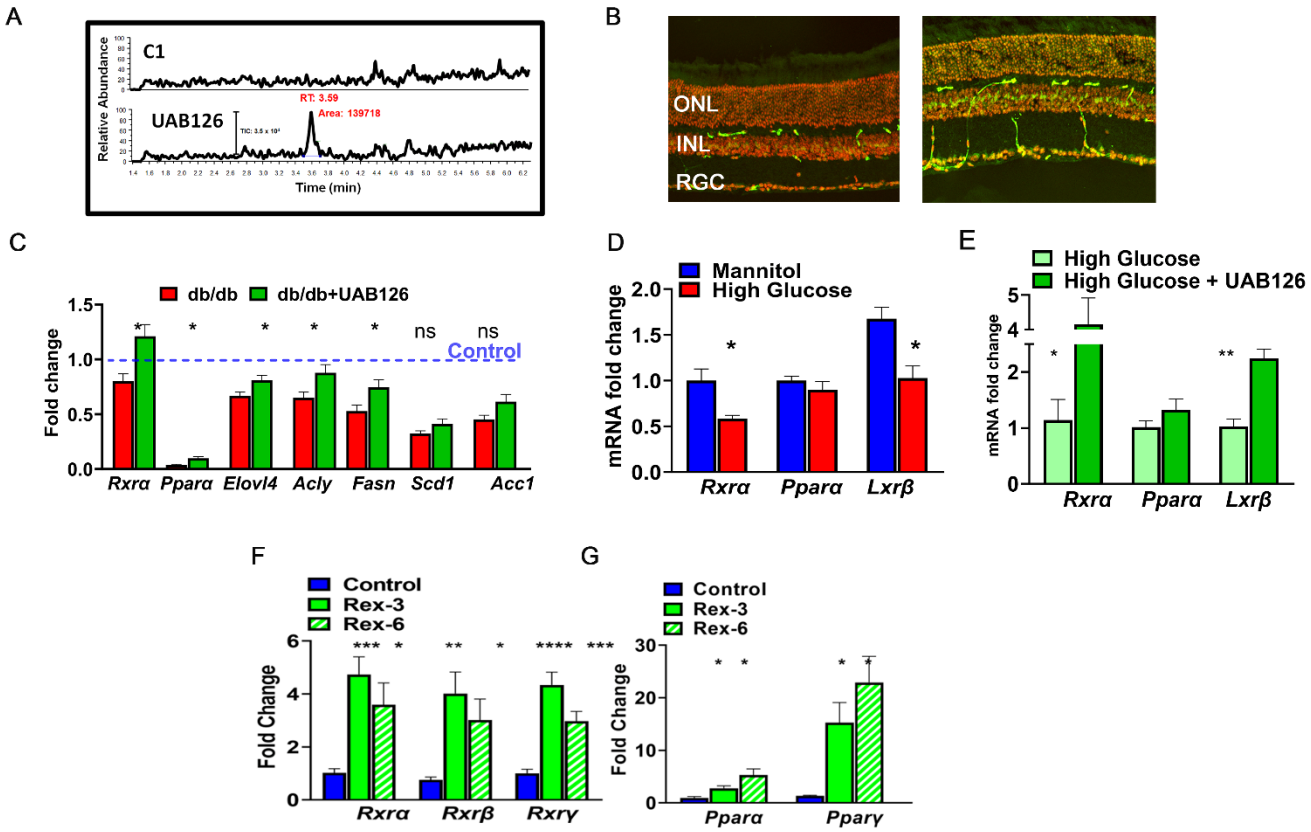

Figure 5. The eye drops containing UAB126 were designed for topical application and retinal delivery of rexinoids. **A:** LC-MS/MS analysis confirms the accumulation of UAB126 in the retinas after topical application of eye drops. LC-MS/MS spectrograms show UAB126-treated retinas compared to untreated controls. **B**: Immunostaining of control (left) and diabetic (right) retinas with anti-RXR antibody detects the RXR signal (in green) following topical UAB126 application. **C:** Topical UAB126 application results in an increase in Rxrα, Pparα, and lipid-associated gene expression in db/db retinas, suggesting altered lipid metabolism in treated diabetic retinas (n=3-5). **D**: Retinal explants cultured in high glucose medium as compared to control (mannitol) exhibit decreased expression of Rxrα, Pparα, and Lxrβ mRNA. **E**: Treatment with UAB126 in high glucose medium increases the expression of these genes (n=3-4). **F**: The application of other rexinoids (rexinoid 3 and rexinoid 6) to C57BL6 retinal explants exposed to high glucose results in a dramatic increase in all three RXR isoforms (n=3-4). **G**: In addition to RXR, UAB126 treatment induces an increase in *Pparα* and *Pparγ* mRNA expression, suggesting potential interactions and effects on other binding partners for RXR-based therapy (n=4). *p < 0.05, **p < 0.01, ***p < 0.001, and ****p < 0.0001.